

Interference Reduction in Wireless Passive Sensor Networks Using Directional Antennas

Abolfazl Razi
ECE Dept. University of Maine
Email: arazi@eece.maine.edu

Ali Abedi
ECE Dept. University of Maine
Email: abedi@eece.maine.edu

Abstract—In this paper, we study a Wireless Passive Sensor Network (WPSN) that employs binary coded differential delay line surface acoustic wave (SAW) devices to monitor temperature in a harsh conditioned environment. The sensors are individually addressed by different reflector patterns. The number of sensors in the system is related to the coded reflectors pattern length which itself is limited by the size constraint of sensors. We propose a new sectorized system model for the WPSN by utilizing a phased circular antenna array to increase the number of sensors in the system that yields higher sensing spatial accuracy. Moreover, the sensing accuracy is further improved by a new two-step detection procedure that purifies the response signal and removes the interference of undesired sensors¹.

Index Terms— Wireless sensor network, passive sensors, SAW device, interference reduction.

I. INTRODUCTION

Surface Acoustic Wave (SAW) devices have been widely used in remote sensing with one to one communication links, but not in Wireless Passive Sensor Networks (WPSN). These passive sensors are useful where the use of battery-powered sensors is not feasible due to harsh environmental conditions [1]. Various parameters including temperature, humidity, stress, and pressure can be measured by observing the change in response signal of SAW devices [2].

SAW devices are battery-free, long lasting, rugged sensors that are implemented in different sensing technologies including (i) *Resonators*, (ii) *Delay lines* and (iii) *Reflective delay lines* [3]. In this paper we, will focus on temperature sensing using binary coded reflective delay lines that can be individually accessed by DS-CDMA codes in a multiple access fashion.

Two main difficulties of using SAW devices as passive sensors are their short distance range and limited addressability. The distance range of these devices is in the range of couple of meters and is mainly imposed by the material, implementation, size and design of the device as well as the interrogation technique [3]. The study of this issue is out of the scope of this paper. The system capacity is defined as the number of devices that can be monitored by a single interrogator system, and depends on different parameters such as available frequency band, desired sensing intervals and accuracy [4].

¹This work is financially sponsored by National Aeronautics and Space Administration (NASA) grant number EP-11-05-5404438. Authors are with Wireless Sensor Networks Laboratory (WiSe-Net) at Electrical and Computer Engineering Department, University of Maine, Orono, ME 04469, USA.

In analogy to active Wireless Sensor Network (WSN), different techniques including TDMA, FDMA/ODFMA, and CDMA/TCDMA are used to increase the capacity of a PWSN. In this paper, we will investigate this issue for binary coded delay line SAW devices interrogated by CDMA coded BPSK signals [5], [6]. A number of modifications are proposed on the interrogator side to improve the system capacity without any change in sensor fabrication process.

The rest of this paper is organized as follows. In section II, the operation of binary coded delay line SAW device as a passive sensor temperature is briefly reviewed. In section III, a system model using directional antennas is proposed. In section IV, a new two-step detection procedure is studied followed by the conclusion in section VI.

II. BINARY CODED DIFFERENTIAL DELAY LINES

A. Basic Operation

A block diagram of a differential delay line SAW device used as a passive sensor is presented in Fig. 1. Each device is composed of an antenna, an Inter Digital Transducer (IDT), two series of reflectors with mirrored pattern, all printed on a temperature sensitive substrate such as $YZ - LiNbO_3$.

The interrogating ElectroMagnetic (EM) wave, is received by the antenna and is converted to an acoustic wave by the IDT. The acoustic waves propagates on the substrate surface in two directions with a velocity in order of 10^5 times slower than the velocity of EM waves in the air. In order to have high efficiency in conversion of EM to acoustic wave the distance between IDT fingers called 'grating period' should be half the wavelength [7]. Consequently, this distance which is a fabrication parameter defines highest applicable frequency as

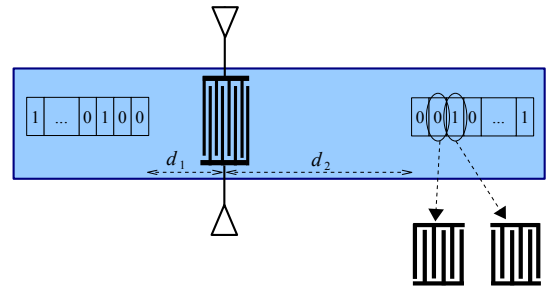


Fig. 1. Binary CDMA coded delay line SAW Device used as a passive temperature sensor.

$$p = \lambda/2 = \frac{V_s}{2f_0} \quad (1)$$

where V_s is the velocity of acoustic wave, f_0 is the interrogator signal central frequency, and p is grating period.

Neglecting the second order effects and inter-finger reflections, with a good approximation the interrogator EM sinusoidal pulse $S_e(t)$ is converted to a acoustic wave $X_a(t)$ with the same central frequency and slightly bigger width that propagates through device surface.

$$X_e(t) = \sin(2\pi ft)R_{\tau_1}(t) \rightarrow X_a(x, t) \approx \alpha [\sin(2\pi f(t - x/V_s))R_{\tau_1+\tau_2}(t - x/V_s) + \sin(2\pi f(t + x/V_s))R_{\tau_1+\tau_2}(t + x/V_s)] \quad (2)$$

where α is fabrication dependent coupling factor, $R_{\tau_1}(t)$ is a rectangular pulse with width τ_1 , and τ_2 is the IDT impulse response width which is related to the number of IDT fingers m with $\tau_2 = \frac{m\lambda}{V_s}$.

Now let us consider a series of reflectors on the substrate surface. According to Fig. 1, reflectors have inter finger distances equal to that of the IDTs. Reflectors have two types corresponding to digits '0' and '1'. In a type '0' reflector, fingers with the odd numbers are connected to the upper line and the fingers with even numbers are connected to the lower line, while it is the reverse in a type '1' reflector. Therefore, an acoustic wave propagating through different types of reflectors generates a voltage signal between upper and lower line of the reflector with 180° phase difference for type '0' and '1' reflectors. Since the reflectors are left open in the employed SAW devices, the induced voltage between reflector fingers regenerate new acoustic waves that propagate in two directions. The regenerated wave's amplitude in the employed SAW devices, based on the experimental results, is almost 0.3 of the incident wave amplitude [5].

Consequently, if we have a surface wave $X_a(t)$ with central frequency f_0 and pulse duration equal to $\tau = d_{Ref}/V_s = \tau_1 + \tau_2$ where d_{Ref} is the reflector length. we will have the following regenerated waves for two reflector types:

$$X_a(t) = \sin(2\pi ft)R_\tau(t) \rightarrow \quad (3)$$

$$Y_a(t) \approx \begin{cases} 0.3 \sin(2\pi ft)R_\tau(t) & \text{type '0' reflector} \\ 0.3 \sin(2\pi ft + \pi)R_\tau(t) & \text{type '1' reflector} \end{cases} \quad (4)$$

For BPSK modulated interrogation signal, type '1' reflectors flips the digits while type '0' reflector keeps the digits unchanged. If the interrogator signal conveys binary stream $\mathbf{x} = \{x_1, x_2, \dots, x_n\}$ and the reflector pattern on the SAW device is $\mathbf{r} = \{r_1, r_2, \dots, r_n\}$, the resulting output stream $\mathbf{y} = \{y_1, y_2, \dots, y_{2n-1}\}$ will be the convolution of these two bit streams.

The above statement is true, if we consider only one phase of the regeneration procedure. In fact, the traveling

acoustic waves induce voltage on the reflectors and the induced voltages regenerate new acoustic waves, and this procedure continues again and again until the induced voltage amplitude is negligible. For instance, if the regeneration amplitude factor is 0.3, considering three regeneration phases, yields a good approximation with error of less than $\sum_{k=3}^{\infty} 0.3^k \approx 4\%$.

The actual behavior of the reflectors are much more complex and includes some other second order effects. For instance, the impulse response of IDT and reflectors are not pure rectangular shaped sinusoidal pulse and contains higher order harmonics. Furthermore, the substrate is limited in dimensions and reflections from the surface ends generate new interfering waves. In this paper, we will consider up to three regeneration phases and neglect all the other second order terms for simplicity.

B. Temperature Sensing by Differential Delay Lines

In the employed sensors, we have two reflector series with mirrored pattern at two sides of the IDT. The interrogator signal is a BPSK modulated DS-CDMA bit stream with the time reversal pattern of the sensor's reflector pattern. Therefore, each reflector series generates an impulse like response signal with a peak at the middle, and the total response signal for the employed differential SAW device has two peaks mixed up with a background pseudo random noise. Also, the response signal for the undesired sensor with a different reflector pattern looks like a random noise. An example of a simulated response signals for the desired and undesired sensor with 31 bit long patterns are depicted in Fig. 2. This simulation is confirmed by the experimental results reported in [5].

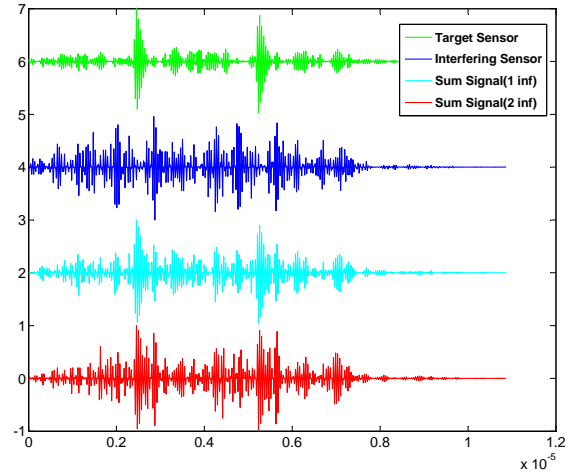


Fig. 2. Response signal of a target and interfering sensors with 31 bit coded reflector pattern interrogated by a time reversal matched signal.

If the physical distances of two reflector series from the IDT is d_1 and d_2 , the time between two peaks, τ_{pp} in the response signal is

$$\tau_{pp}(T) = 2[d_1(T) - d_2(T)]/V_s(T) \quad (5)$$

where T is temperature. The distance between IDT and reflectors and also acoustic wave velocity on the device depends on the temperature [8], therefore the change on the time distance between the two peaks indicates the temperature change according to (6).

$$\frac{\Delta\tau_{pp}}{\tau_{pp}} = TCD \cdot \Delta T \quad (6)$$

where ΔT is temperature change and TCD is temperature coefficient of time delay. It is notable that the impulse response of IDT and reflectors are also dependent on the temperature since inter finger distances changes with the temperature, but this change has less effect compared to the change in peak location and is not considered in this work.

C. Multiple Access

The maximum number of sensors in a system monitored by an interrogator is limited by the number of codes that we can have for the reflector patterns with acceptable autocorrelation to cross-correlation ratio. For a binary coded SAW device with n_R reflectors at each side, it is obviously much less than 2^{n_R} . The number of reflectors in each device is limited by the size constraint of the sensors as well as the attenuation caused by each reflector. Hence, in a practical application, good codes can be chosen based on the system SNR level. In our system model, we have 16 codes with length of 31 bits chosen from all 2^{31} codes by an extensive computer search.

III. SENSING NETWORK STRUCTURE

We assume that the sensors are uniformly spaced on a circle to monitor the temperature of a circular area around the interrogator as depicted in Fig. 3.

Higher spatial sensing accuracy can be obtained by utilizing more sensors. The idea is to increase the number of sensors in the system by inter-sensor interference reduction that can be achieved by employing directional antennas.

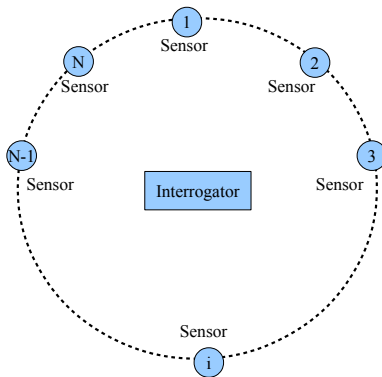


Fig. 3. System model: sensors are placed in a circle with an interrogator in the middle.

To get a symmetric radiation pattern, we chose uniform spaced circular antenna array with the specifications presented in Table I.

TABLE I
CIRCULAR ARRAY ANTENNA PARAMETERS

Parameter	Value
Antenna Length	$\lambda/2$
Spacing	$\lambda/4$
Current distribution	Chebyshev
Sweeping mode	Phase
Number of elements	16
Active elements	4

The array includes $n_A = 16$ elements, where only $n_E = 4$ elements are active at each time instant. The 3rd order *chebyshev* polynomial $T_3(x) = 4x^3 - 3x$ is chosen for current amplitudes to minimize the side lobe level for a given main lobe width. In this equation, we have $x = x_0 \cos(kd_A \cos(\phi/2))$ where k is wave number and x_0 is defined by the desired side lobe level R_0 using $x_0 = \cosh(\frac{1}{3} \cosh^{-1}(R_0))$ equation. Spacing parameter is chosen as $d_A = \lambda/4$ to guarantee one-side radiation [9]. The reflector plate is modeled as a wire grid plane. The design is based on the approximation that the four adjacent elements form a linear antenna array and the resulting pattern is confirmed by *4nec2* software and is depicted in Fig. 4.

Fig. 4 demonstrates that the -6db main lobe width of the radiation pattern is $W_{6db} \approx 60^\circ$. Hence, the system can be sectorized into $S = 360^\circ/W_{6db}$ sectors and we can reuse the sensors with the same code pattern by angular spacing equal or more than W_{6db} that increase the number of sensors by a factor of 6.

Using smaller sectors with narrower main lobe width, increases the number of sensors and hence provides higher spatial accuracy. On the other hand, this increases the number of interrogation phases that results in a longer time interval between consequent sensor interrogations.

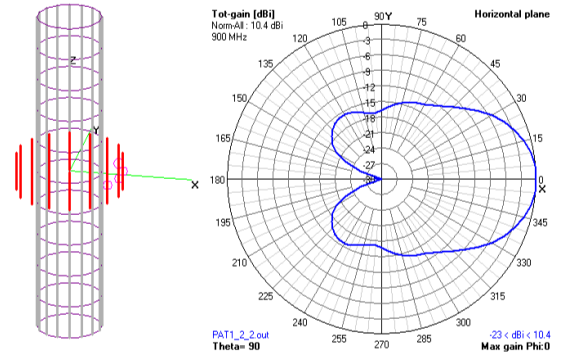


Fig. 4. Circular uniform spaced antenna array with chebyshev current amplitudes.

IV. DETECTION PROCEDURE

Although the number of sensors in the system may be significantly increased using directional antennas, but still interference exist especially among the sensors response signal inside the main lobe. For instance, Fig.2 presents the target sensor response, an interfering sensor response, and the target sensor response signal mixed up with one and two interfering sensors signal. It is clear from the figure, that when more than

two sensors interfere with the target sensor, the peaks buried in the noise and sensing procedure base on the traditional peak search techniques fails.

In this section, we propose the idea of intelligently removing undesired interference terms from the response signal to improve the system performance compared to the currently used blind autocorrelation methods. The two step interrogation procedure is run for any sector.

A. Initialization phase

In this phase, we try to recognize the system configuration. To do so, we setup a look up table \mathcal{K} for each sector that contains all the possible codes. Then we interrogate the sensors in this sector with all possible codes. For any code, that the total response signal is an impulse like signal with two peaks in the middle, we mark the existence of a sensor with this specific code in the lookup table. The distance between peaks gives us a rough estimation of the temperature sensed by this sensor. At the end of initialization step, the lookup table includes all the codes corresponding to the existing sensors in the sector. Since the initialization phase runs only once or less frequently, it is not time sensitive and can be done with much narrower radiation pattern main lobe width to achieve higher certainty in the system configuration.

B. Interrogation phase

Interrogation phase is performed in a repeated manner. In this phase, each sensor is individually interrogated by a signal with the corresponding code pattern. The response signal is received by the interrogator and is stored to be analyzed. The response signal $y_i(t)$ includes the response from the target sensor mixed up with the undesired response signals from the other sensors in the sector as well as noise term as

$$y_i(s_i, t) = x_i(t) * \sum_{k \in \mathcal{K}} [a_k h_k(s_k, t) + n_k(t)] + n(t) \quad (7)$$

where $x_i(t)$ is the interrogator signal with time reversal code, a_k is the equivalent path coefficient between the interrogator and the k^{th} sensor considering both directions, $h_k(s, t)$ is the k^{th} sensor impulse response with sensing parameter s_k (temperature T_k in our case), $n_k(t)$ is the noise term of the k^{th} sensor, and $n(t)$ is the noise at the interrogating receiver.

The configuration information extracted at the initialization phase can be used to more accurately localize the peaks in the signal in the following manner. First, we estimate the response from any of the present undesired sensors with considerable interference level. To do so, we calculate the expected response signal for each of the interfering sensors. Then we estimate the path gain for each sensor by correlating the response signal with the expected signal. The correlation should be maximized by checking response signals corresponding to different sensing parameter values, s_k . Then this signal is reduced from the received signal to remove the interference signal of this sensor. This procedure is performed for all the sensors in the sector. Then the resulting signal is interference free or interference-lowered signal and includes the desired

signal with a random noise. Now we can find the maximum peak locations that identifies the temperature sensed by this specific sensor. This procedure is presented in Fig. 5. The detailed results will be provided in follow-up papers.

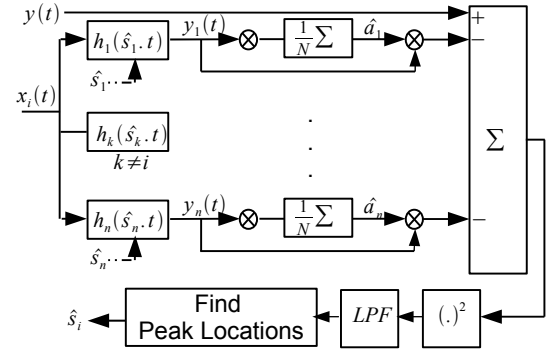


Fig. 5. Block Diagram of the receiver with new detection method

V. CONCLUSION

In this paper, a new method is proposed to increase the accuracy of a WPSN employing binary coded delay line SAW devices for temperature monitoring. The number of sensors can be significantly increased by sectorizing the monitoring area using directional antennas that enables us to reuse the equi-pattern sensors in different sectors. A new two-step detection procedure is introduced to recognize the existing sensors in each sector and intelligently remove their interfering signal from the response signal of the target sensor. This method provides higher accuracy of peak detection compared to the traditional autocorrelation techniques. The cost paid is higher complexity and longer interrogation time. This solution makes the procedure an appropriate choice for WPSNs with unknown configuration or even moving sensors.

VI. ACKNOWLEDGMENT

The authors would like to sincerely thank Dr. John Vetelino and Dr. Herbert M. Aumann for his thoughtful comments in array antenna design.

REFERENCES

- [1] O. Akan, M. Isik, and B. Baykal, "Wireless passive sensor networks," *Communications Magazine, IEEE*, vol. 47, no. 8, pp. 92–99, 2009.
- [2] L. Reindl, G. Scholl, T. Ostertag, H. Scherr, U. Wolff, and F. Schmidt, "Theory and application of passive saw radio transponders as sensors," *Ultrasonics, Ferroelectrics and Frequency Control, IEEE Transactions on*, vol. 45, no. 5, pp. 1281–1292, Sep. 1998.
- [3] G. Scholl, C. Korden, E. Riha, C. Ruppel, U. Wolff, G. Riha, L. Reindl, and R. Weigel, "Saw-based radio sensor systems for short-range applications," *Microwave Magazine, IEEE*, vol. 4, no. 4, pp. 68–76, 2003.
- [4] G. Ostermayer, A. Pohl, L. Reindl, and F. Seifert, "Multiple access to saw sensors using matched filter properties," in *Ultrasonics Symposium, 1997. Proceedings., 1997 IEEE*, vol. 1, Oct. 1997, pp. 339–342 vol.1.
- [5] E. Dudzik, A. Abedi, D. Hummels, and M. Pereira da Cunha, "Wireless sensor system based on saw coded passive devices for multiple access," 2008, pp. 1116–1119.
- [6] A. Razi, F. Afghah, and A. Abedi, "Hierarchical network development of wireless passive sensors," in *Fly by Wireless Workshop (FBW), 2010 Caneus*, 2010, pp. 30–31.
- [7] O. Schwelb, E. Adler, and J. Slaboszewicz, "Modeling, simulation, and design of saw grating filters," *Ultrasonics, Ferroelectrics and Frequency Control, IEEE Transactions on*, vol. 37, no. 3, pp. 205–214, May 1990.
- [8] J. Kuypers, L. Reindl, S. Tanaka, and M. Esashi, "Maximum accuracy evaluation scheme for wireless saw delay-line sensors," *Ultrasonics, Ferroelectrics and Frequency Control, IEEE Transactions on*, vol. 55, no. 7, pp. 1640–1652, 2008.
- [9] J. D. Kraus, *Antennas for all applications*. McGraw-Hill, 2004.